Universal Journal of Electrical and Electronic Engineering 5(1): 9-19, 2017 http://www.hrpub.org
DOI: 10.13189/ujeee.2017.050102

Design of a Broadband Planar RF Structure for a 0.22 THz Travelling Wave Tube

Vishnu Srivastava*, Deepak Sharma

Microwave Tubes Division, CSIR-Central Electronics Engineering Research Institute, India

Abstract Planar broadband THz travelling wave tube is being designed for ultra broadband high speed data rate communication and imaging. A simplified analytical approach is developed for designing of a planar staggered double vane rectangular waveguide slow-wave structure (SDVSWS) for a broadband 0.22 THz 100W TWT. The structure is inherently compatible for sheet beam operation, and it is designed for an electron beam of voltage 20 kV and current 50 mA. 3D e.m. field simulator code CST-MWS was used for simulating the SDVSWS using the analytical design parameters. It is found that the dispersion characteristic by the analytical method matches well within 5% with the simulated dispersion characteristic of the structure. Effects of various parameters of a double-vane SWS on dispersion and impedance characteristics are evaluated for achieving a planar TWT of bandwidth more than 40 GHz with high gain. It is shown that pitch and vane height are most significant parameters and half-period staggering of double vanes in the structure provides wider bandwidth, high impedance and high symmetric RF electric field for efficient beam-wave interaction.

Keywords Planar RF Structure, Vane Loaded Rectangular Waveguide, Slow Wave Structure, THz Travelling Wave Tube, Vacuum Electronic Devices

1. Introduction

High power terahertz frequencies from 0.1 THz to 10 THz of the electromagnetic spectrum are being explored for numerous scientific and technological applications like ultra-broadband communication, security, medical imaging, remote sensing, planetary exploration and spectroscopy [1-5]. Ultra broadband communication and sensing applications demand extremely broad bandwidth (>10 GHz) and high power (>10 W) linear devices at THz frequencies. Solid-state devices are not capable to amplify output power more than few mW at THz frequencies. Efficient and compact vacuum electronic devices (VEDs) can amplify tens of watts output power at THz frequencies. Design and development of VEDs for THz frequencies are extremely challenging because of small size of parts having dimensions in hundreds of microns with tolerance less than ten microns and surface roughness less than hundred nano-meter. Among various vacuum tube amplifiers, travelling wave tubes (TWTs) are most preferred choice as a high power THz amplifier for communication and sensing applications due to their high beam-wave energy conversion efficiency over an extremely wide bandwidth, large RF thermal capacity and high gain amplification at THz frequencies. TWTs can have amplified output power in tens of watts at such high frequencies with gain more than 20 dB and efficiency around 5-10%.

Major components of a THz TWT, are electron gun with cathode for an electron beam of suitable shape and size; RF slow-wave structure (SWS) with input and output RF couplers; a magnetic field circuit for focusing of an electron beam propagating from electron gun to the collector; depressed collector for recovering energy from the spent electron beam; and finally packaging with conduction or radiation cooling. TWT is designed and fabricated for a desired RF performance like output power, gain, efficiency, AM/PM factor, phase shift, inter-modulation components, and gain compression over the desired operating band.

TWT with planar RF structure and sheet beam is preferred at THz frequencies because planar structure is easier to fabricate using MEMS technologies and sheet beam has higher beam current capacity as compared to pencil beam. Sheet beam has very small space charge force as compared to a pencil beam of same beam current. A simplified analytical approach is developed for design of a wideband planar RF SWS of a THz TWT. Analytical design is presented in section 2, for a 0.22 THz TWT as frequency band around 0.22 THz offers significant advantages for communication, radar, and other applications because of wide atmospheric spectral window from 0.2 THz to 0.3 THz. The analytical design of the planar RF structure for a 0.22 THz TWT is evaluated using 3D electromagnetic field

simulator. The simulation results are presented in section 3.

2. Analytical Design of Planar RF SWS

For a TWT of centre frequency 0.22 THz and output power 100W, the electron beam of beam voltage 20kV and beam current 50mA is selected considering electronic efficiency around 10%. Important planar RF SWS that are recently being reported for a 0.22-THz TWT are: (i) staggered double-vane loaded rectangular waveguide SWS [6-10], (ii) meander line loaded rectangular waveguide SWS [11], (iii) Sine waveguide SWS [12], (iv) corrugated waveguide SWS [13], (v) H-plane and E-plane loaded rectangular waveguide SWS [14], (vi) single and double grating type SWS [15-16]. The staggered double-vane (on E-plane) loaded rectangular waveguide SWS, as shown in Fig.1 for a unit cell, is selected for the present design of a wideband 0.22 THz 100W TWT because it has wide bandwidth and high interaction impedance. Also, it has low circuit loss and it is convenient to fabricate.

There are nine design parameters of a staggered double vane rectangular waveguide SWS for a given beam voltage. These parameters, as shown in Fig.1, are: pitch of the vanes (p), staggering factor (d), gap between two vanes (g), vane shape (vs), vane thickness (t), vane height (l), beam tunnel height (2a), total height (h), and width (w) of the rectangular waveguide. The vane-loaded rectangular waveguide SWS is a forward-fundamental structure and first forward space harmonic (n=+1) of phase shift per pitch varying from 2π to 3π is selected for amplification operation. Although the interaction impedance of higher space harmonic is less but it provides wider operating bandwidth and larger size of the structure for given operating beam voltage. The beam voltage is selected for the synchronous condition with the wave at centre frequency 0.22 THz corresponding to phase shift per pitch equals to $(2\pi+0.5\pi)$.

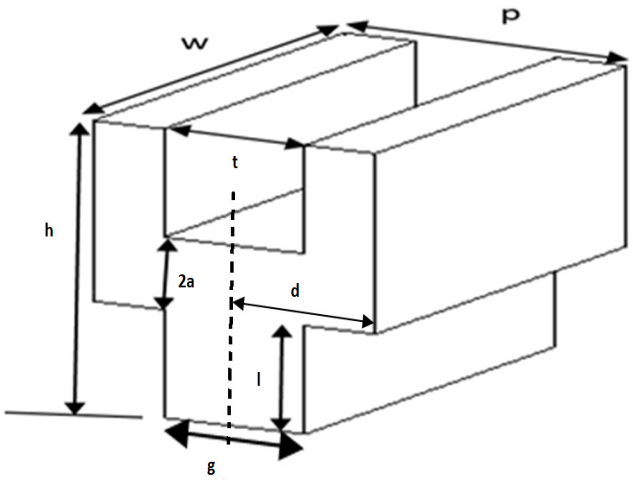

Figure 1. Unit cell of a staggered double-vane SWS

Pitch p of the vane-loaded structure is determined from the phase shift per pitch at centre frequency 0.22 THz, using equation (1).

$$\beta p = 2.5\pi \quad (1)$$

where, β is the axial propagation constant and is given by:

$$\beta = \omega/vp \quad (2)$$

ω is the angular frequency and vp is the phase velocity which is taken as beam velocity (u_0) because of beam-wave synchronism condition in a TWT.

Beam velocity is determined from beam voltage (V_0) in kV, using equation (3) [8]:

$$u_0 = [c \sqrt{(1- 1/ (1 + (V_0/511))^2)}] \quad (3)$$

Beam velocity is obtained as 8.15×10^7 m/s.

Pitch of the vane structure is, therefore, determined as: p=463 μm for 20 kV beam voltage and centre frequency 0.22 THz.

Gap (g) between two adjacent vanes on same side of waveguide is decided by equation (4):

$$g/p = 0.3 \quad (4)$$

This condition is decided on the basis of the high impedance of the structure. Gap (g) is therefore chosen as 139 μm.

Rectangular shape vanes are used because of simplicity in fabrication and considering mechanical and thermal aspects. Vane thickness (t) is decided from pitch and gap, using equation (5):

$$t = p – g \quad (5)$$

This gives, t=324 μm.

Beam tunnel height (2a) is determined by the condition of high interaction impedance of the structure, using equation (6):

$$\beta a = 1.0 \quad (6)$$

giving, 2a=118 μm.

Vane height should be maximum possible for high impedance of the structure. Vane height (l) is selected by equation (7) for high impedance of the structure:

$$(l/2a) = 3.0 \quad (7)$$

giving, l= 354 μm.

The total height (h) of the structure is therefore taken as:

$$h = [2(l + a)] \quad (8)$$

giving, h = 826 μm.

Total height (h) of the structure also decides the upper end cut-off frequency of the waveguide structure. It corresponds to the resonant frequency of a unit cell.

Width of the structure (w) decides the lower cut-off frequency (f_c) of the dispersion curve which corresponds to the cut-off frequency of the dominant TE_{10} mode of the rectangular waveguide of broader dimension w. Therefore, structure width (w) is determined by using equation (9):

$$fc = c / 2w \quad (9)$$

Width (w) of the structure is selected as 770 μm that gives

fc = 194.67 GHz. For centre frequency 220 GHz, cold bandwidth is 50.66GHz, and upper cutoff frequency is 245.33GHz.

For the beam tunnel size 118 μm x 770 μm of the designed SWS, sheet beam is chosen of maximum rectangular size of 100 μm x 700 μm. It gives current density 71.4 A/cm^2, for beam voltage 20 kV and beam current 50 mA. The rectangular waveguide of input and output couplers are selected compatible with the standard rectangular waveguide (WR-3) of dimension (864 μm x 432 μm) [17]. The designed structure is matched with the standard waveguide at the input and the output ends by tapering the height and pitch of the vanes for wideband matching. The analytically designed parameters of unit period of the vane-loaded structure are summarized in Table 1. These parameters are compared with the parameters as reported by Deng [9] and Ryskin [10] for their 0.22-THz TWTs. The vanes are taken of rectangular shape and vanes on the opposite sides are staggered by half of the period (d=p/2) for wide bandwidth and high impedance of the vane-loaded SWS. This was demonstrated in section 3, by simulation.

Table 1. parameters of a unit cell of the SWS

Parameter	Analytical Design (μm)	Deng[9] (μm)	Ryskin [10] (μm)
Pitch [p]	463	450	500
Gap[g]	139	113	250
Vane thickness[t]	324	337	100
Beam Tunnel [2a]	118	110	200
Vane height[l]	354	300	300
W/G height [h]	826	710	800
W/G width [w]	770	770	850
Staggering [d]	p/2	p/2	p/2
Vane shape	Rectangular	Rectangular	Rectangular

3. Simulation Using 3D EM Code

The analytically designed SWS of section 2, is simulated using 3D electromagnetic field simulator code CST-MWS [18]. One cell of the periodic structure (Fig.1) of dimension as given in Table 1, is simulated using CST-MWS. In CST-MWS, eigen mode solver with hexahedral meshing and AKS algorithm method are selected. Simulation is carried out for forward space harmonic (n=+1) varying phase shift per period (βp) from 2π to 3π, as shown in Fig.2.

Dispersion curves for mode 1 and mode 2 of the staggered double-vanes structure with 20kV beam velocity line are shown in Fig.2. Mode 1 is nearly from 194 GHz to 254 GHz, mode 2 is nearly from 254 GHz to 274 GHz, and 20 kV electron beam line intersects the dispersion curve of mode 1 at 212 GHz. The lower end frequency of mode 1 at phase shift 2π, corresponds to the cut-off frequency of the dominant mode TE10 of the rectangular waveguide of width (w). The upper cut-off frequency of the pass band characteristic of mode 1 at phase shift 3π is decided by the resonant frequency of unit cell of the structure.

Fig.3a shows comparison between dispersion curves of vane-loaded structure with and without half-period staggering in the vanes. It shows that half period staggering of vanes provides widest possible bandwidth with high interaction impedance. Fig.3b shows pierce interaction impedance curve for mode 1.

The simulated values of cold bandwidth, lower cut-off frequency (f_c) and upper cut-off frequency (f_v), and the central frequency are comparable with the analytically decided values as discussed in section 2. Comparative values are shown in Table 2.

Table 2. Analytical and CST-MWS parameters comparison

Parameter	Analytical Value	CST-MWS value
βp at 220GHz	2.5 π	2.5551 π
f_c	194.67 GHz	194.49 GHz
bandwidth	50.66 GHz	45 GHz un-staggered 59 GHz staggered

Field patterns (E-field) of mode 1 at 0.22 THz for the non-staggered and the staggered double-vane structure are shown in Fig.4a and Fig.4b, respectively for a phase shift per period of 120 degrees. Non-staggered structure has an out-of-phase axial electric field variation along transverse direction (anti-symmetric) in a unit cell (Fig.4a). This leads to non-synchronous interaction of the electron beam with the RF wave. Whereas in the half period staggered structure, the π phase shift between the two TE mode vane arrays effectively constitutes a wide passband structure with symmetric axial fields as shown in Fig.4b. This field interacts constructively with the electron beam and provides high interaction impedance. Because of wide bandwidth and high impedance, staggered double-vane structure is used.

4. Parametric Analysis

The effects of varying various parameters on dispersion and impedance characteristics of the structure are simulated using CST-MWS simulator. The designed planar SWS is analyzed by ±10% variation in different parameters. Their effects on the dispersion and impedance characteristics are presented.

Figure 5 shows the effect of varying circuit pitch keeping gap between two vanes constant, i.e., varying vane thickness. The reduced pitch increases resonant frequency of the unit cell that is related to the increase in the upper end frequency of the pass band. Therefore, the bandwidth of the structure increases with decrease in circuit period. Bandwidth increase due to reduction of pitch is related with a reduction of the circuit impedance, as shown in Fig. 5b. On the other end at the operating frequency 0.22THz, decrease in pitch is related

to the increase of phase shift per pitch that leads to reduced phase velocity, and reduced interaction impedance. Similar effects are observed on the dispersion and the impedance curves varying pitch and correspondingly varying vane gap keeping vane thickness constant. In this case also, the bandwidth is increased and circuit impedance is reduced with decrease in pitch with corresponding decrease in the gap.

The effect of beam tunnel height is analysed: (i) keeping total height constant and varying vane height accordingly with the beam tunnel height, and (ii) total height is varied accordingly with the beam tunnel height keeping vane height constant. In the first case the cold bandwidth is increased significantly, as shown in Fig. 6. In this case also, the upper cutoff frequency is increased with increase in beam tunnel height that is again related to the increase of the resonant frequency of unit cell.

Effect of varying both vane height (l) and waveguide width (w), keeping other dimensions' constant is analyzed. The dispersion curves are shown in Fig.7 for different values of l and w. Here, both the lower and the upper end frequencies are affected. The bandwidth is increased with decrease in l (caused by increase of the upper end frequency that is related to the resonant frequency of unit cell), and with increase in w (caused by reduction of the lower end frequency that is related to the cut-off frequency of the rectangular waveguide). It shows that vane height is to be less and waveguide width is to be more for wider bandwidth of the double-vanes SWS.

The effects of waveguide width on the bandwidth and impedance are simulated, as shown in Fig.8. Fig.8a shows dispersion curves and Fig.8b shows impedance curves for different width of the structure. Operating band shifts to higher frequency and bandwidth decreases with a decrease in the width of the structure.

The effects of one conducting slab and two conducting slabs [14] on the H-plane of the double-vane rectangular waveguide, are simulated. Size of the conducting slab is taken: height 100 μm, thickness 40 μm and width 110 μm. Fig.9a and Fig.9b shows dispersion and impedance curves. Conducting slab on H-plane decreases bandwidth by shifting lower end frequency, as shown Fig.9a.

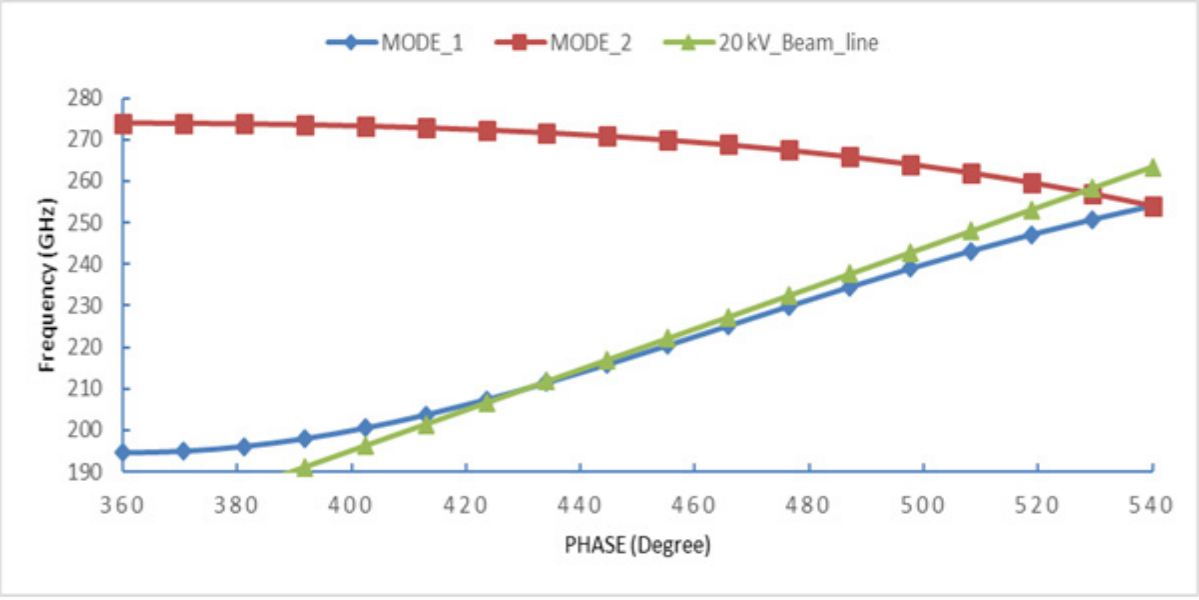

Figure 2. Dispersion curves for mode 1 and mode 2 with 20kV beam line

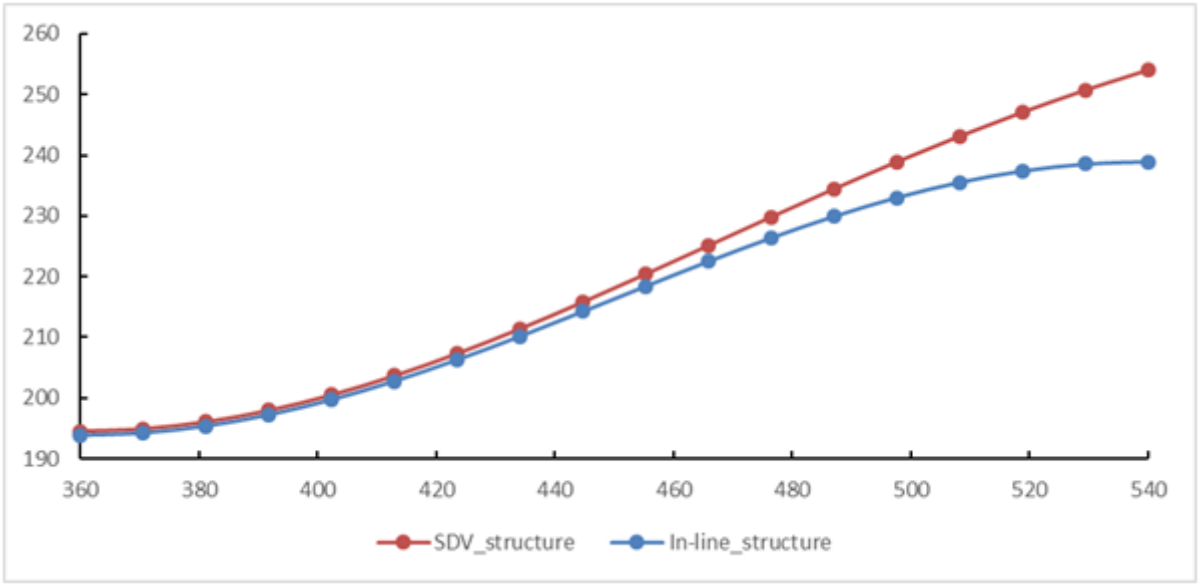

Figure 3a. Dispersion curves without and with half-period staggered double-vane SWS.

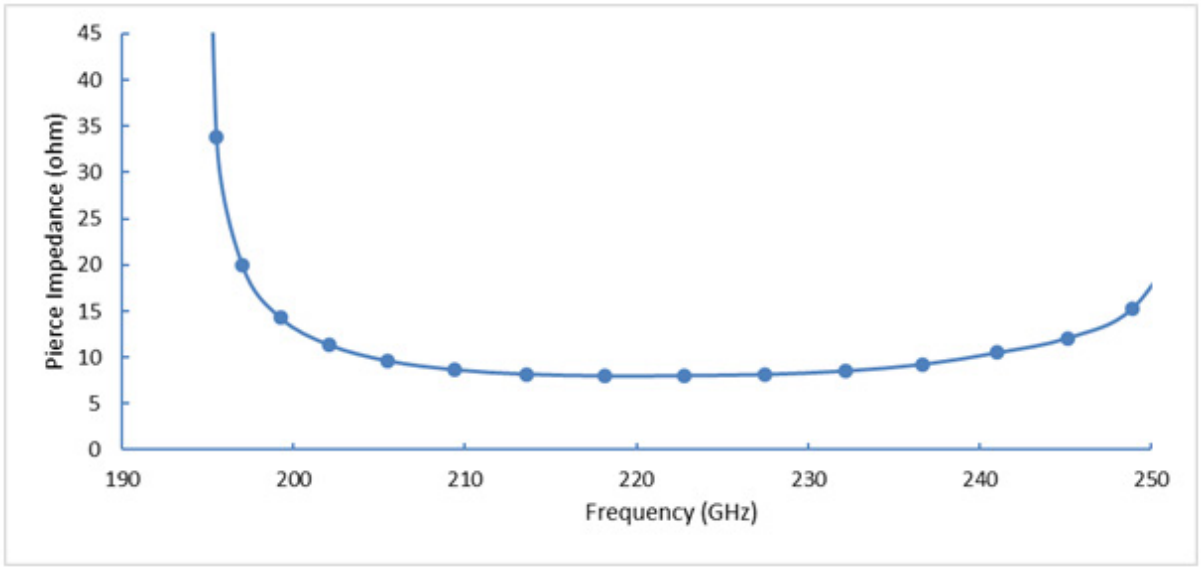

Figure 3b. Interaction Impedance curve for mode 1

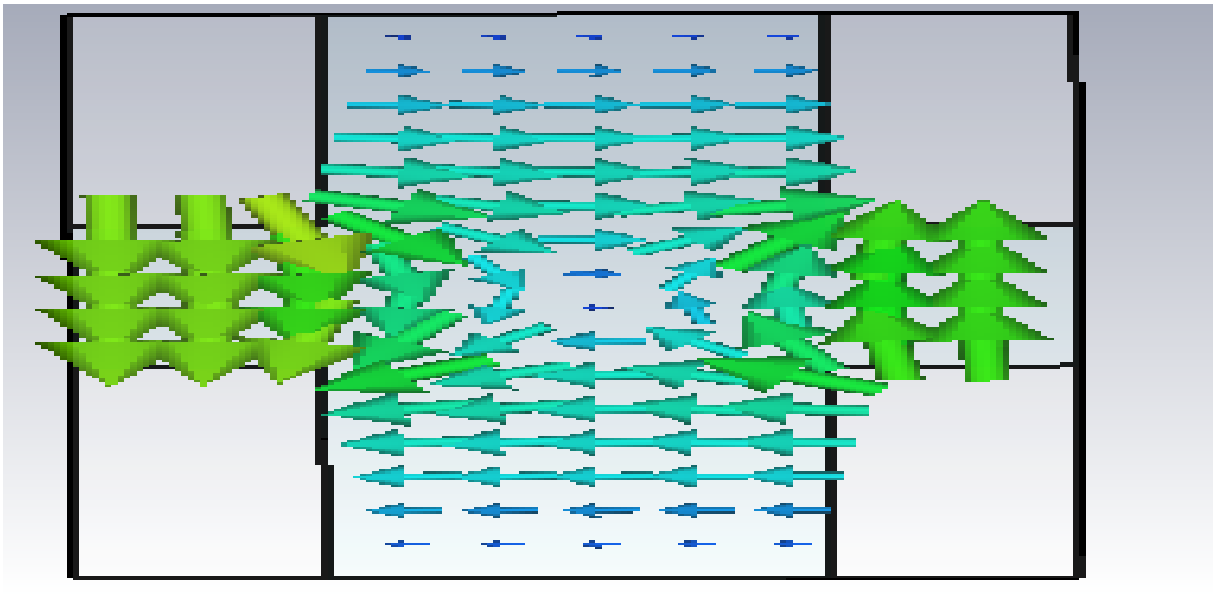

Figure 4a. E-field for non-staggered double-vane SWS

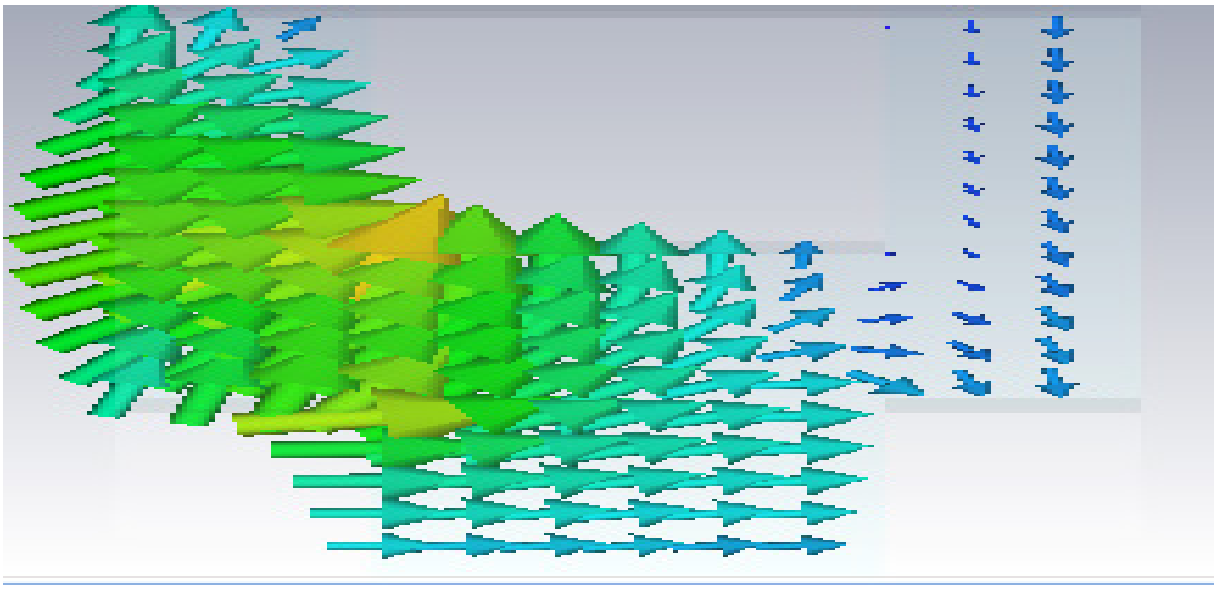

Figure 4b. E-field for staggered double-vane SWS

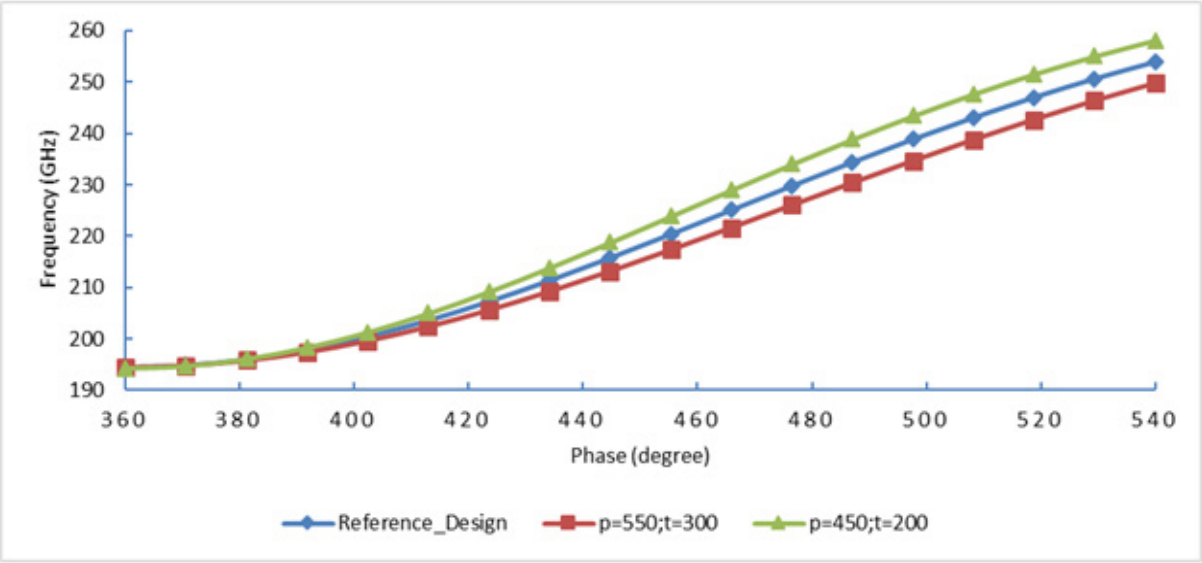

Figure 5(a). Dispersion curves for change in pitch (p) and vane thickness (t) for same gap between vanes (g)

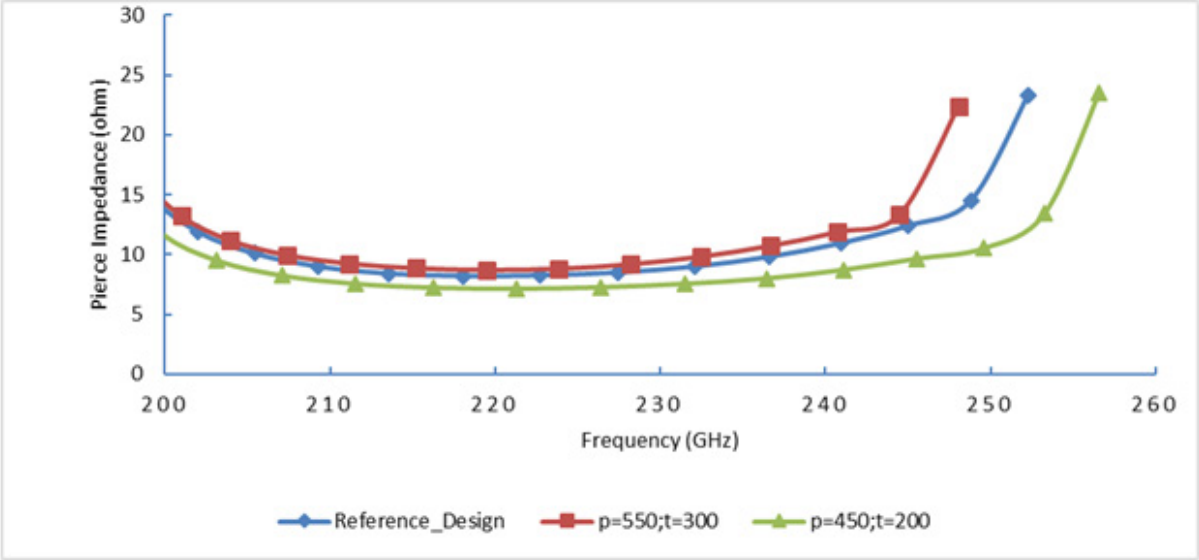

Figure 5(b). Impedance curves for change in pitch (p) and vane thickness (t) for same gap between vanes (g)

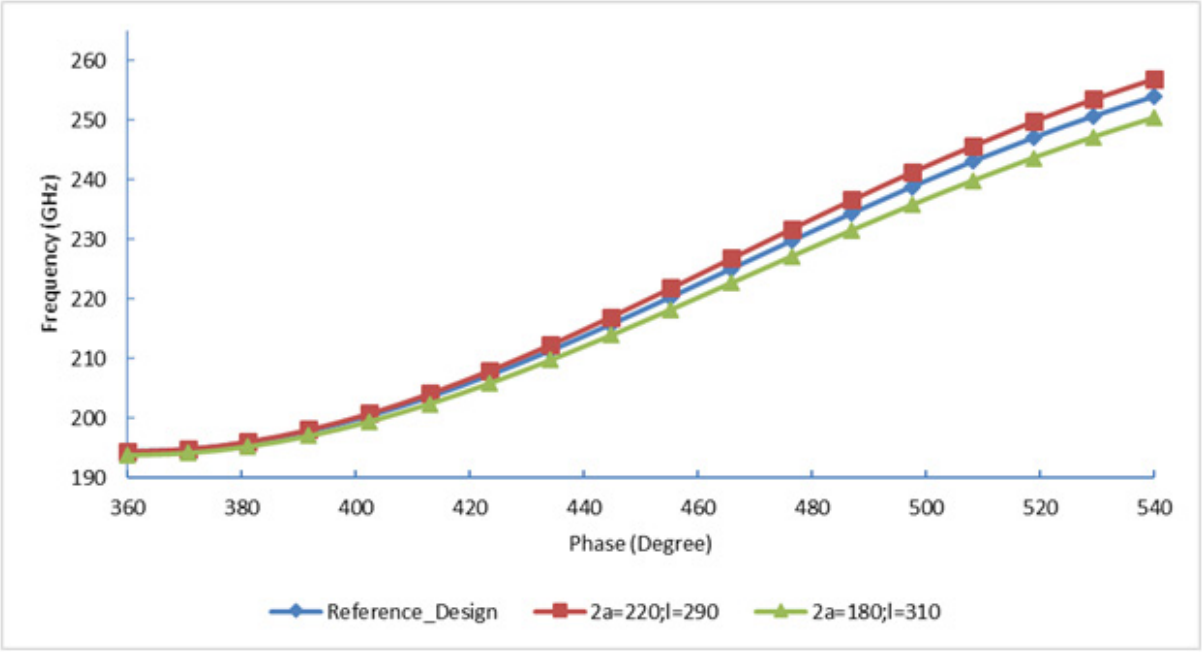

Figure 6. Dispersion curves for change in beam tunnel height (2a) and vane height (l)

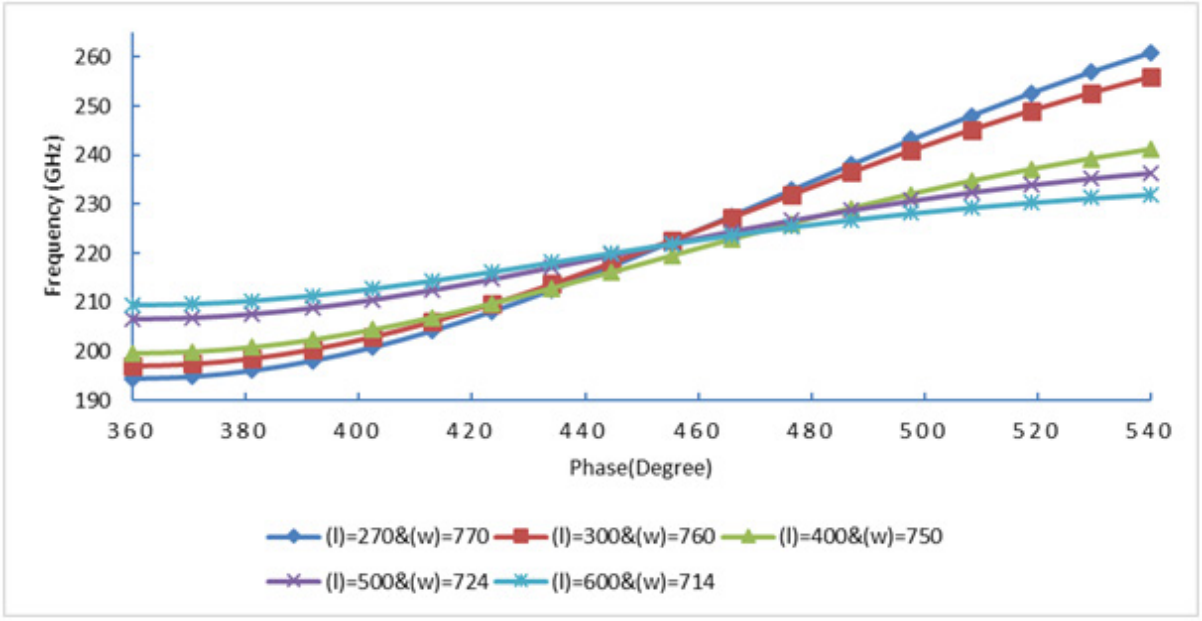

Figure 7. Dispersion curves varying vane height (l) and width of the structure (w)

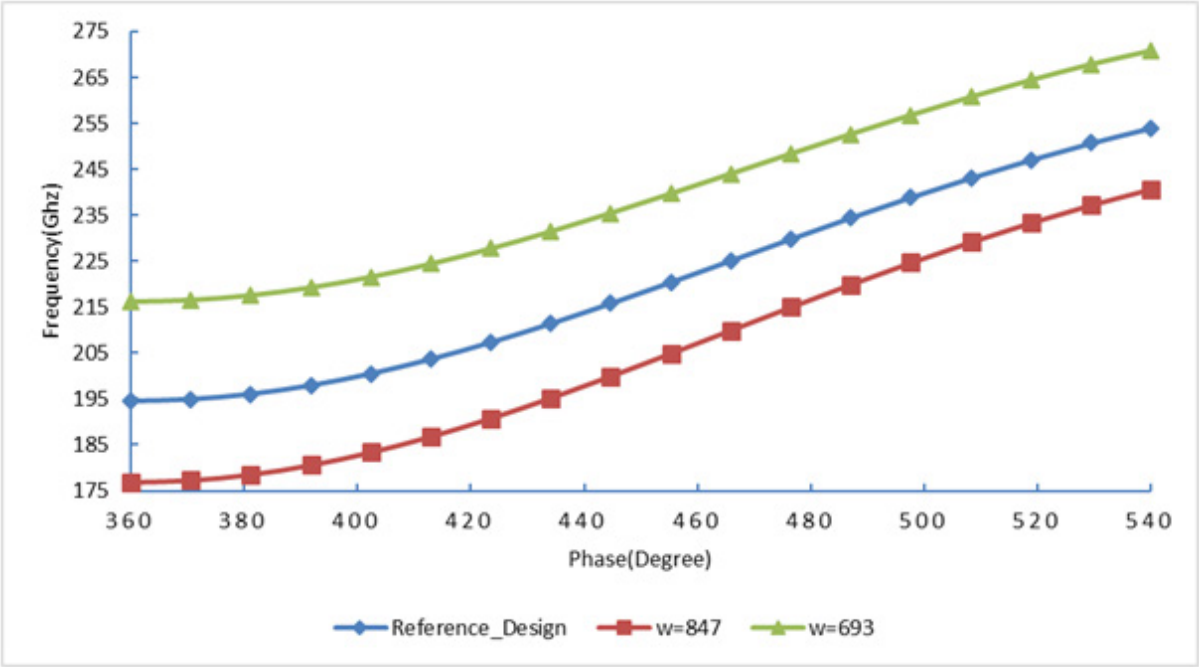

Figure 8(a). Dispersion curves for change in width of the structure (w)

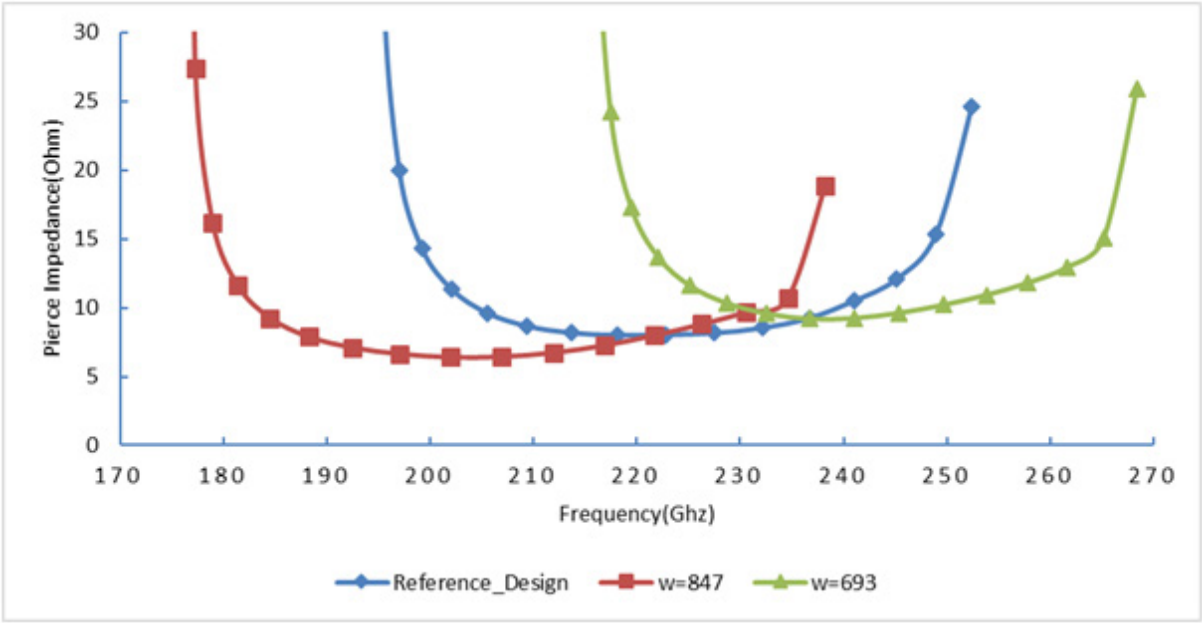

Figure 8(b). Impedance curves for change in width of the structure (w)

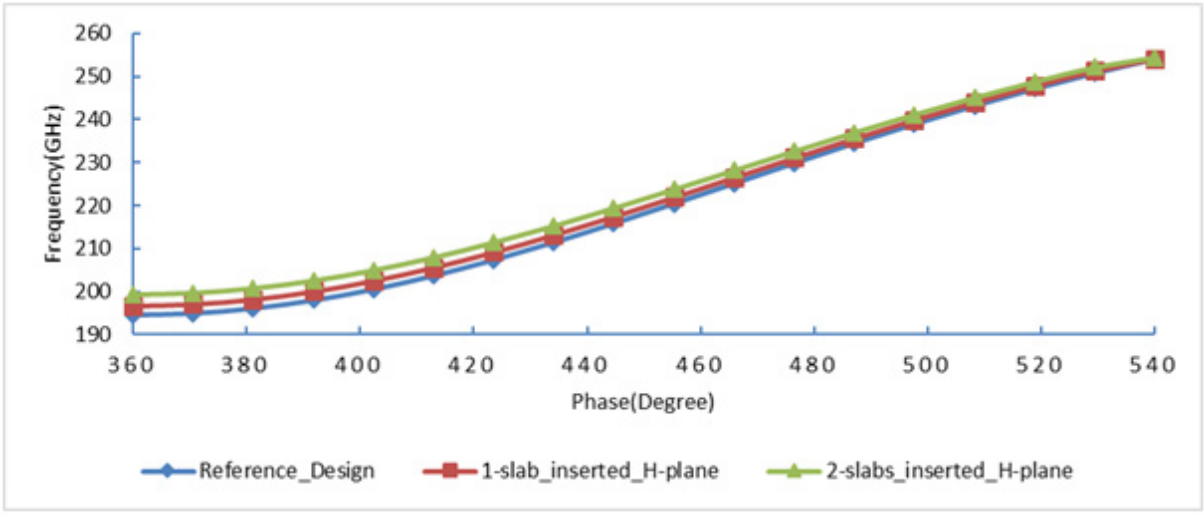

Figure 9(a). Dispersion curves with and without slabs in H-plane of the staggered double-vane SWS

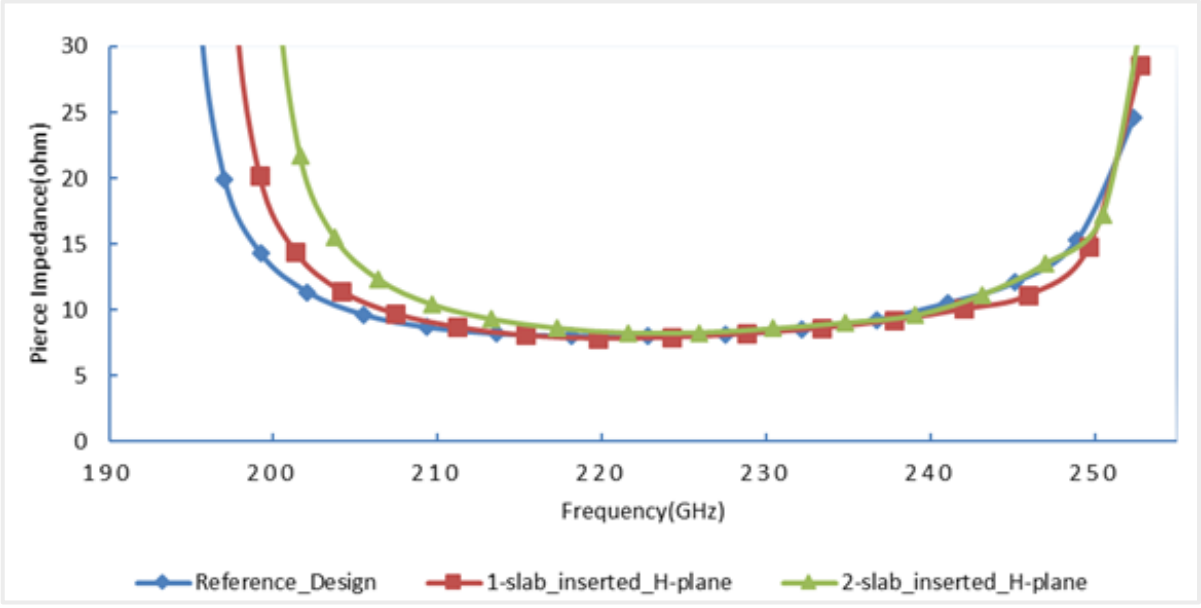

Figure 9(b). Impedance curves with and without slabs in H-plane of the staggered double-vane SWS

Effects of ±10% variation in the various parameters on the change in the bandwidth and interaction impedance characteristics at 0.22 THz are summarized in Table 3.

Table 3. Effect of ±10% variation in parameters on bandwidth and impedance

s/n	±10% variation in the parameter	Change in Bandwidth GHz	Change in Impedance ohms
1.	period [for same gap]	-8.4	+1.6
2.	period [for same vane thickness]	-10.5	+8.8
3.	beam tunnel [for same total height]	+6.5	-3.4
4.	beam tunnel [for same vane height]	+1.4	-3.9
5.	Vane height [for same tunnel height]	-12.9	+1.5

Variations of all parameters like vane period, vane height, vane thickness, beam tunnel height, gap length have significant effects on dispersion and impedance characteristics. Therefore, all parameters of a structure are to be optimized as per the requirement of bandwidth and gain. The RF performance like output power, gain, bandwidth, efficiency, for a 0.22 THz 100W TWT using the designed double-vane SWS and 20kV, 50mA sheet beam are being analysed using our in-house developed SUNRAY codes [19-20] for large-signal analysis of TWT. These results will be presented in our next paper.

5. Conclusions

Broadband high power high gain TWT of 0.22 THz centre frequency is of significant importance for ultra-broadband

high data rate wireless communication and imaging because of the available atmospheric spectral window over wideband from 0.20 THz to 0.30 THz. Compact 0.22 THz TWT of 100 W output power, 20 dB gain, 10% beam efficiency and 30 GHz bandwidth is being investigated. Slow-wave structure is the most critical component of a TWT because it decides the rf performance of a device. There is a need to design SWS of wide bandwidth, high interaction impedance, and that is easy to fabricate through micro fabrication technologies with high precision (dimension tolerance <2μm) and high surface finish (roughness <100nm). Staggered double-vane rectangular waveguide slow-wave structure is identified for the 0.22 THz TWT. Simplified analytical design approach is presented for design of SDV-SWS. This structure has large bandwidth of more than 50GHz and high interaction impedance. The analytical design of a SDV-SWS for the 0.22 THz TWT was validated against a standard 3D e.m. field simulator CST-MWS. Effects of various parameters on dispersion and impedance characteristics are analyzed, and it is concluded that the pitch and vane height are two critical parameters significantly affecting the structure bandwidth.

Acknowledgements

Authors are thankful to the CSIR, New Delhi for their research funding, and to the Director, CSIR-CEERI, Pilani for his support. They are also thankful to their colleagues of MWT division for helpful interactions. Deepak Sharma is also thankful to the Director, CSIR-NPL, New Delhi, where he has joined w.e.f. 1st Jan 2017.

REFERENCES

[1] J H Booske, Vacuum electronic high power THz sources, IEEE Transactions on Terahertz Science and Technology, vol.1, no. 12, 54-75, 2011.

[2] M J Rosker and H B Wallace, Vacuum Electronics and World Above 100 GHz, IEEE International Vacuum Electronics Conference (IVEC), California, PL (3), 1-6, 2008.

[3] V Srivastava, THz vacuum microelectronic devices, Journal of Physics, Conference Series, 114 (12015), 1-10, 2008, DOI:10.1088/1742-6596/114/1/012015.

[4] J F Federici, B Schulkin, F Huang, D Gary, F Oliveira and D Zimdars, THz imaging & sensing for security applications - explosives, weapons and drugs, Semiconductor Science Technology, vol. 20, 266–280, 2005.

[5] H Jin Song, T Naatsuma, Handbook of terahertz technologies: devices & applications, Pan Stanford, ISBN 9789814613088, 2015.

[6] Y M Shin, System Design Analysis of 0.22 THz Sheet-Beam TWTA, IEEE Transaction, vol. ED-59, no. 1, 1792-98, 2012.

[7] Y M Shin, L R Barnett, N C Luhmann, Phase shifted TWT for Ultrawideband high power submillimeter wave generation, IEEE transaction on electron devices, vol. 56, no. 5, 2009.

[8] Y M Shin, A Baig, L R Barnett, N C Luhmann, Modeling Investigation of an Ultrawideband Terahertz sheet beam TWT Amplifier, IEEE trans., vol. ED58, no.9, 3213-18, 2011.

[9] G Deng, P Chen, J Yang, Z Yin, J Ruan, 0.22 THz two stages cascaded staggered double-vane TWT, J Comput Electron, 15:634-638 DOI 10.1007/S 10825-015-0774-1, 2016.

[10] Nikita M. Ryskin, Development and Modelling of a Sheet-Beam, Sub-THz Travelling Wave Tube, IEEE International Vacuum Electronics Conference, Beijing, 2015.

[11] A I Benedik, A G Rozhnev, N M Ryskin, G V Torgashov, Study of Electrodynamic Parameters of the planar Meander Slow wave structures for THz Band TWTs, IEEE International Vacuum Electronics Conference, Beijing, 2015.

[12] X Xu, Y Wei, F Shen, Z Duan, Y Gong, H Yin and W Wang, Sine Waveguide for 0.22-THz Travelling Wave Tube, IEEE Electron Device Letters, vol. 32, no.8, 1152-54, 2011.

[13] C Paoloni, M Mineo, Double Corrugated Waveguide for G-Band TWTs, IEEE Trans., vol. ED 61, no.12, 4259-64, 2014.

[14] L R Billa, M N Akram and X Chen, H-Plane and E-Plane Loaded Rectangular Slow-Wave Structure for Terahertz TWTA, IEEE Trans., vol. ED 63, no. 4, 1722-27, 2016.

[15] C D Joye, J P Calame, M Garven, D Park and B Levush, Microfabrication of 220 GHz Grating for Sheet Beam Amplifier, IEEE-IVEC, 2010.

[16] B E Carlsten, S J Russell, F L Krawczyk and S Humphries, Technology Development for a mm-Wave Sheet-Beam TWT, IEEE Trans. on Plasma Science, vol. 33, no. 1, 85-93, 2005.

[17] Waveguide frequency bands with interior dimensions, Online available from www.miwv.com

[18] CST Microwave Studio, Online available from www.cst.com

[19] V Srivastava, 1-dimensional & 2.5-dimensional Large Signal Analysis of a helix TWT, 24th International Journal of Electronics & Communication Technology, vol.4, 2013.

[20] V Srivastava, M Latha, P C Panda, D Maurya, S Aditya, Analysis of different structures TWTs using SUNRAY-1D and SUNRAY 2.5D codes, IEEE International Vacuum Electronics Conference, Beijing, 2015.